



OCT 8 1952

NACA TN 2800

# NATIONAL ADVISORY COMMITTEE FOR AERONAUTICS

TECHNICAL NOTE 2800

SOLUTIONS OF LAMINAR-BOUNDARY-LAYER EQUATIONS WHICH  
RESULT IN SPECIFIC-WEIGHT-FLOW PROFILES LOCALLY  
EXCEEDING FREE-STREAM VALUES

By W. Byron Brown and John N. B. Livingood

Lewis Flight Propulsion Laboratory  
Cleveland, Ohio



Washington  
September 1952

FOR REFERENCE

NOT TO BE TAKEN FROM THIS ROOM

NACA LIBRARY  
LANGLEY AERONAUTICAL LABORATORY  
Langley Field, Va.

## TECHNICAL NOTE 2800

SOLUTIONS OF LAMINAR-BOUNDARY-LAYER EQUATIONS WHICH RESULT IN SPECIFIC-  
WEIGHT-FLOW PROFILES LOCALLY EXCEEDING FREE-STREAM VALUES

By W. Byron Brown and John N. B. Livingood

## SUMMARY

Solutions of the laminar-boundary-layer equations when large temperature changes in the boundary layer and large pressure changes in the main stream occur simultaneously were found to be very sensitive to the behavior of the third-order derivative of the boundary-layer stream function as the specific weight flow approached its free-stream value. (The specific weight flow is proportional to the first derivative of the stream function.) Theoretically, all derivatives of the specific weight flow should vanish at the outer edge of the boundary layer; however, in numerical solutions, only a restricted number of these conditions can be applied. Under assumed constant wall temperature and small Mach numbers, solutions of the laminar-boundary-layer equations for stream-to-wall temperature ratios of 2 and 4, Euler numbers of 0.5 and 1, and rates of cooling-air flow through the porous wall signified by values of the coolant flow parameter of 0, -0.5, and -1 previously reported did not fulfill the condition that the third-order derivative of the stream function vanish at the outer edge of the boundary layer. New solutions which not only fulfilled this condition but also which resulted in very small values of higher-order derivatives were therefore obtained. The resulting specific-weight-flow, velocity, and temperature distributions and the local heat-transfer coefficients are tabulated and are compared with those determined previously. Friction coefficients and dimensionless displacement, momentum, convection, and thermal boundary-layer thicknesses are also tabulated.

The new solutions resulted in specific weight flows which exceeded the free-stream values. These excesses ranged from 2 percent for the impermeable wall, a stream-to-wall temperature ratio of 2, and an Euler number of 0.5 to 15 percent for the permeable wall with a coolant flow parameter of -1, a stream-to-wall temperature ratio of 4, and an Euler number of 1, the most severe case considered.

## INTRODUCTION

General solutions of the laminar-boundary-layer equations are obtainable for free-stream velocity distributions which are proportional to a power of the distance from the stagnation point and which are found in incompressible flow around infinite wedges. These wedge solutions have proved useful as good approximations for other types of flow (reference 1) and have served as a basis for methods of determining local heat-transfer coefficients for bodies of arbitrary shape (references 2 and 3).

Wedge solutions were first presented in reference 4 for conditions of constant property values and small Mach numbers. Extension to high-speed flow is accomplished in reference 5, in which the wedge solutions are used to approximate heat transfer to bodies of arbitrary shape. Reference 6 includes the effects of aerodynamic heating. Extensions to include variable wall temperatures are made in references 7 and 8.

In reference 9, the effects of transpiration cooling are included for constant property values, constant wall temperature, and small Mach numbers. The extension to include variable fluid properties is presented in references 1 and 10.

Tables of laminar-boundary-layer solutions with variable fluid properties and a pressure gradient in the main stream are given in reference 10 for conditions of constant wall temperature and small Mach numbers. When large temperature changes occurred in the boundary layer and were accompanied by large pressure changes in the main stream, a new type of velocity profile not found in any of the earlier referenced work was sometimes obtained. In particular, when the wall was four times as hot as the stream and a stagnation-point pressure gradient was present, the velocity increased very rapidly from zero at the wall to a value 20 percent above the free-stream value one-third of the way through the boundary layer and then decreased gradually to the free-stream value as the boundary-layer density approached the stream value. This behavior is explained by E. R. G. Eckert to be caused by the fact that the warmer layers in the boundary layer are more accelerated than the outside flow because of their lower density when both are subject to the same pressure drop.

In view of this result, an examination of the tabular distributions of reference 10 was made to determine whether some temperature- and pressure-drop effect could be found in the opposite case, that is, when the boundary layer was much cooler than the free stream and consequently denser. This, it was thought, might cause the specific weight flow (product of density and velocity) to exceed the free-stream value near the wall because of the high density value there. When this alternative

was inserted in the analysis by permitting the specific weight flow to exceed its free-stream value and to decrease toward it until the profile became horizontal for the second time, it was found to fit well and to yield a smoother blending of the boundary-layer and the free-stream values of specific weight flow, temperature, and velocity than that of reference 10 in which the free-stream value of the specific weight flow was attained but not exceeded when the profile became horizontal the first time. At this point the curvature of the specific-weight-flow profile did not approach zero as the slope did when large pressure gradients in the main stream and strong cooling occurred together. In all other cases considered, the specific-weight-flow profile curvature did approach zero.

Accordingly, 12 cases of reference 10 that involved cooling at the wall combined with large pressure gradients in the main stream were recalculated at the NACA Lewis laboratory; these new solutions, for which the second- and higher-order derivatives of the boundary-layer stream function vanish at the outer edge of the boundary layer are presented herein. Stream-to-wall temperature ratios of 2 and 4, Euler numbers (nondimensional pressure gradient parameter) of 0.5 and 1, and nondimensional flow rates through the porous walls of 0, -0.5, and -1 were used in these recalculations. It should be noted that distributions presented in reference 10 for an Euler number of 0.4 would likewise be revised by the present method. These revised values were not calculated, however, because it was believed that the Euler numbers 0.4 and 0.5 were not sufficiently far apart to justify the recalculation. Velocity, specific-weight-flow, and temperature distributions are tabulated as well as the dimensionless stream function of Falkner and Skan and its derivatives and the dimensionless temperature function of Pohlhausen and its derivatives.

For each case, dimensionless forms of displacement, momentum, convection, and thermal boundary-layer thicknesses, Nusselt numbers, and wall friction coefficients are given.

### SYMBOLS

The following symbols are used in this report:

C                    constant of proportionality

$$C_{f,w} = \frac{\tau_w}{\frac{\rho_w U_\infty^2}{2}}$$

$c_p$                   specific heat at constant pressure

Eu	Euler number, $\frac{-x \frac{dp}{dx}}{\rho_{\infty} U_{\infty}^2}$ ; $U_{\infty} = Cx^{Eu}$
f	dimensionless stream function
f', f'', f'''	first, second, and third derivatives of f with respect to $\eta$
H	heat-transfer coefficient
k	thermal conductivity
Nu	Nusselt number, $\frac{Hx}{k_w}$
P	$\frac{T}{T_w} = 1 + \theta \left( \frac{T_{\infty}}{T_w} - 1 \right) = P$
Pr	Prandtl number, $\frac{c_{p,w} \mu_w}{k_w}$
p	pressure
Re	Reynolds number, $\frac{U_{\infty} \rho_w x}{\mu_w}$
T	fluid temperature
$T_w$	refers to wall temperature and coolant upon emergence from porous wall
U	fluid velocity at edge of boundary layer
u	fluid velocity parallel to wall in boundary layer
v	fluid velocity normal to wall in boundary layer
x	distance along surface
y	distance normal to surface
$\alpha$	exponent of temperature for specific heat, $c_p \propto T^{\alpha}$
$\delta^*$	displacement boundary-layer thickness

$\delta_c$	convection boundary-layer thickness
$\delta_i$	momentum boundary-layer thickness
$\delta_t$	thermal boundary-layer thickness
$\epsilon$	exponent of temperature for thermal conductivity, $k \propto T^\epsilon$
$\eta$	dimensionless boundary-layer coordinate, $y \sqrt{\frac{\rho_w U_\infty}{\mu_w x}}$
$\theta$	temperature-difference ratio, $\frac{T - T_w}{T_\infty - T_w}$
$\theta', \theta''$	first and second derivatives of $\theta$ with respect to $\eta$
$\mu$	absolute viscosity of fluid
$\rho$	density of fluid
$\tau_w$	shear stress at wall
$\psi$	stream function
$\omega$	exponent of temperature for viscosity, $\mu \propto T^\omega$
Subscripts:	
w	wall
$\infty$	main stream

## ANALYSIS

### Laminar-Boundary-Layer Equations

The equations of the laminar boundary layer for steady-state flow of a viscous fluid with heat transfer, presented in references 1 and 10 and repeated for convenience herein, are

Momentum equation:

$$\rho u \frac{\partial u}{\partial x} + \rho v \frac{\partial u}{\partial y} = \frac{\partial}{\partial y} \left( \mu \frac{\partial u}{\partial y} \right) - \frac{\partial p}{\partial x} \quad (1)$$

Continuity equation:

$$\frac{\partial}{\partial x} (\rho u) + \frac{\partial}{\partial y} (\rho v) = 0 \quad (2)$$

Energy equation:

$$c_p \left( \rho u \frac{\partial T}{\partial x} + \rho v \frac{\partial T}{\partial y} \right) = \frac{\partial}{\partial y} \left( k \frac{\partial T}{\partial y} \right) + \mu \left( \frac{\partial u}{\partial y} \right)^2 + u \frac{\partial p}{\partial x} \quad (3)$$

The boundary conditions are

$$u = 0, v = v_w, \text{ and } T = T_w \text{ when } y = 0$$

and

$$\left. \begin{aligned} u \rightarrow U_\infty; \frac{\partial u}{\partial y} \rightarrow 0, \frac{\partial^2 u}{\partial y^2} \rightarrow 0; \dots \frac{\partial^n u}{\partial y^n} \rightarrow 0 \\ T \rightarrow T_\infty; \frac{\partial T}{\partial y} \rightarrow 0, \frac{\partial^2 T}{\partial y^2} \rightarrow 0; \dots \frac{\partial^n T}{\partial y^n} \rightarrow 0 \end{aligned} \right\} \quad (4)$$

when  $y \rightarrow \infty$

#### Assumptions

For simplification of the analysis, the following assumptions are made:

- (1) The Mach number is small.
- (2) The Euler number is constant.
- (3) The wall temperature is constant.

(4) The fluid property variations are expressible in terms of the absolute temperature as follows:

$$\mu \propto T^\omega \quad k \propto T^\epsilon \quad c_p \propto T^\alpha \quad \rho \propto T^{-1} \quad (5)$$

The second and third terms in the right member of equation (3) are proportional to  $M^2$  and hence approach zero as  $M^2$  does. By virtue of assumption (1), these two terms may be neglected. Furthermore, for the same reason,  $\rho_w$  and  $T_\infty$  are considered constants.

## Transformation to Ordinary Differential Equations

The transformation from partial to total differential equations is accomplished by the change in variables

$$\left. \begin{aligned} \eta &= y \sqrt{\frac{\rho_w U_\infty}{\mu_w x}} \\ \theta &= \frac{T - T_w}{T_\infty - T_w} \\ f &= \frac{\rho_w \psi}{\sqrt{\mu_w x U_\infty \rho_w}} \end{aligned} \right\} \quad (6)$$

where  $\eta$  is the dimensionless independent variable introduced by Blasius and  $f$  and  $\theta$  are the dimensionless dependent variables representing the stream function and the temperature, respectively.

Substitution of  $\eta$ ,  $f$ , and  $\theta$  in the partial differential equations, use of the abbreviation  $P = \frac{T}{T_w} = 1 + \theta \left( \frac{T_\infty}{T_w} - 1 \right)$ , and the simplifying assumptions yield (references 1 and 10) the energy equation

$$-\theta'' = \frac{Eu + 1}{2} Pr_w P^{\alpha - \epsilon} \theta' f + \epsilon \left( \frac{T_\infty}{T_w} - 1 \right) P^{-1} \theta'^2 \quad (7)$$

and the momentum equation

$$\begin{aligned} f''' &= Eu P^{-\omega} f'^2 - \frac{Eu + 1}{2} P^{-\omega} f f'' - Eu \frac{T_w}{T_\infty} P^{-\omega - 1} - \\ &\frac{Eu + 1}{2} \left( \frac{T_\infty}{T_w} - 1 \right) P^{-\omega - 1} f f' \theta' - \left( \frac{T_\infty}{T_w} - 1 \right) P^{-1} f' \theta'' - \\ &(\omega + 2) \left( \frac{T_\infty}{T_w} - 1 \right) P^{-1} f'' \theta' - \omega \left( \frac{T_\infty}{T_w} - 1 \right)^2 P^{-2} f' \theta'^2 \end{aligned} \quad (8)$$

The boundary conditions are

$$f' = 0, f = f_w, \text{ and } \theta = 0 \text{ when } \eta = 0$$

and



$$\theta \rightarrow 1; \theta' \rightarrow 0, \theta'' \rightarrow 0, \dots \theta^n \rightarrow 0$$

$$f' \rightarrow \frac{T_w}{T_\infty}; f'' \rightarrow 0, f''' \rightarrow 0, \dots f^n \rightarrow 0 \quad (9)$$

$$\text{when } \eta \rightarrow \infty$$

### Discussion of Boundary Conditions

Satisfying so many boundary conditions simultaneously is difficult. Initial values must be assumed for  $f''$  and  $\theta'$  to begin the calculation; then the step-by-step numerical solution of equations (8) and (9) can be carried out until the boundary layer merges with the free stream. For constant property values,  $T_\infty/T_w = P = 1$  and equation (7) reduces to

$$-\theta'' = \frac{Eu + 1}{2} Pr_w \theta' f$$

Consequently,  $\theta'' \rightarrow 0$  when  $\theta' \rightarrow 0$ . For constant property values, equation (8) reduces to

$$f''' = Eu f'^2 - \frac{Eu + 1}{2} f f'' - Eu$$

and  $f''' \rightarrow 0$  when  $f'' \rightarrow 0$  and  $f' \rightarrow 1$ . The solutions for constant property values can therefore be obtained by adjusting the initial values of  $f''$  and  $\theta'$  at the wall so that, at the free-stream boundary,  $\theta \rightarrow 1$  when  $\theta' \rightarrow 0$  and  $f' \rightarrow 1$  when  $f'' \rightarrow 0$ .

For variable property values, equation (7) shows that  $\theta'' \rightarrow 0$  when  $\theta' \rightarrow 0$ , as before. However, equation (8) reduces to

$$f''' = Eu P^{-\omega} f'^2 - Eu \frac{T_w}{T_\infty} P^{-\omega-1} - \frac{Eu + 1}{2} \left( \frac{T_\infty}{T_w} - 1 \right) P^{-\omega-1} f f' \theta' -$$

$$\left( \frac{T_\infty}{T_w} - 1 \right) P^{-1} f' \theta'' - \omega \left( \frac{T_\infty}{T_w} - 1 \right)^2 P^{-2} f' \theta'^2$$

When  $f'' \rightarrow 0$ , and for  $f''' \rightarrow 0$  it is necessary for  $\theta' \rightarrow 0$ ,  $\theta \rightarrow 1$ , and  $f' \rightarrow \frac{T_w}{T_\infty}$  simultaneously.

According to reference 10,

$$\frac{\rho u}{\rho_{\infty} U_{\infty}} = f' \frac{T_{\infty}}{T_w} \quad (10)$$

so that the specific weight flow is proportional to  $f'$ ; that is, the variation of  $f'$  can be used to measure the variations of the specific weight flow.

Former method. - The solutions reported in reference 10 were obtained by assuming that the free-stream boundary conditions were satisfied when  $f'' \rightarrow 0$  the first time and  $f' \rightarrow T_w/T_{\infty}$ . These calculations show that for the flat plate, where  $Eu = 0$ , the boundary-layer specific weight flow and temperature merge with the free stream at points sufficiently near each other that  $f'''$  is quite close to zero when  $f'' = 0$ . This is likewise true when  $Eu$  has small negative values (adverse pressure gradient).

When the Euler number has large positive values, 0.5 and 1,  $f'$  builds up to the free-stream value  $T_w/T_{\infty}$  very rapidly. For example, when  $f'' = 0$ ,  $f''' = -0.014$  when  $Eu = 1$ ,  $T_{\infty}/T_w = 4$ , and  $f_w = 0$ . If, in addition, there is flow through the porous wall ( $f_w = -1$ ) the situation becomes worse, with  $f''' = -0.042$  when  $f'' = 0$ .

At the free stream, the curvature of  $f'$  should be zero, that is,  $f''' \rightarrow 0$ . The foregoing discussion shows that the method reported in reference 10 does not satisfy this condition sufficiently well for large positive Euler numbers combined with large temperature ratios. Consequently, a modification in the solution for these cases was necessary.

Present method. - In an effort to satisfy the free-stream boundary conditions more accurately for the cases of large positive Euler numbers and temperature ratios,  $f'$  was allowed to exceed the main-stream value and initial values of  $f''$  and  $\theta'$  were adjusted so that  $f' \rightarrow T_w/T_{\infty}$  when  $f'' \rightarrow 0$  the second time. The result of this modification, as will be shown later, was that  $f'''$  approached zero quite closely even for large positive Euler numbers and temperature ratios. Moreover, it will also be shown that  $f''' \rightarrow 0$  at values of  $\eta$  (or  $y$ ) only slightly less than those for which  $\theta'$  approached zero.

#### NUMERICAL CALCULATION AND RESULTS

Equations (7) and (8) were solved with physical properties appropriate for air in the range 600° to 2400° F obtained from logarithmic plots of data taken from reference 11. These values were

$$\text{Pr}_w = 0.7 \quad \omega = 0.7 \quad \epsilon = 0.85 \quad \alpha = 0.19$$

The cases recomputed here are 12 in all as follows:

$$f_w = 0, -0.5, -1$$

$$\frac{T_\infty}{T_w} = 2, 4$$

$$\text{Eu} = 0.5, 1$$

#### Method of Calculation

The system of differential equations (7) and (8) was solved by Picard's method (reference 12). Values of  $f''$  and  $\theta'$  were assumed for  $\eta = 0$  and calculations were carried through the boundary layer until  $f'' \rightarrow 0$  (second time) and  $\theta' \rightarrow 0$ . Here the value of  $f'$  should be  $T_w/T_\infty$  and that of  $\theta$  should be 1. In order to ensure that the higher derivatives also approach zero, the differences in the  $f'''$  and  $\theta''$  columns should be approaching zero. If not, the initial values were adjusted until the desired values at the boundary-layer border were attained.

The velocity and specific-weight-flow distributions were found as in reference 10 by use of the relations

$$\left. \begin{aligned} \frac{u}{U_\infty} &= f' P \\ \frac{\rho u}{\rho_\infty U_\infty} &= f' \frac{T_\infty}{T_w} \end{aligned} \right\} \quad (11)$$

The displacement, momentum, and convection thicknesses were found as in references 1 and 10 by the equations

$$\left. \begin{aligned} \frac{\delta^*}{x} \sqrt{\text{Re}} &= \int_0^\infty \left( 1 - f' \frac{T_\infty}{T_w} \right) d\eta \\ \frac{\delta_1}{x} \sqrt{\text{Re}} &= \frac{T_\infty}{T_w} \int_0^\infty f' (1 - P f') d\eta \\ \frac{\delta_c}{x} \sqrt{\text{Re}} &= \frac{T_\infty}{T_w} \int_0^\infty f' (1 - \theta) d\eta \end{aligned} \right\} \quad (12)$$

Another thickness called the thermal boundary-layer thickness is defined in reference 3 as

$$\delta_t = \int_0^{\infty} \frac{T - T_{\infty}}{T_w - T_{\infty}} d\eta$$

By means of relations (6), this equation can be reduced to the nondimensional form

$$\frac{\delta_t}{x} \sqrt{Re} = \int_0^{\infty} (1 - \theta) d\eta \quad (12a)$$

The specific-weight-flow, velocity, and temperature distributions for each of the 12 cases considered are presented in table I. Also included in table I are the local heat-transfer coefficients and friction coefficients, obtained as in references 1 and 10 from the relations

$$\frac{Nu}{\sqrt{Re}} = \theta'_w$$

and

$$\frac{C_{f,w}}{2} \sqrt{Re} = f''_w$$

and values of the dimensionless displacement, momentum, convection, and thermal boundary-layer thicknesses, obtained by integrations made from the distributions in the tables according to equations (12) and (12a).

Table II is a summary table including local heat-transfer coefficients and friction coefficients and values of the dimensionless displacement, momentum, convection, and thermal boundary-layer thicknesses. This table contains the results presented in reference 10, with corrections made for the 12 cases that were recalculated and reported herein and with the additional values of the dimensionless thermal boundary-layer thickness; all thickness calculations were reviewed, and several minor corrections in addition to the 12 cases referred to previously were included.

In the calculations reported herein, four decimal places were carried in all cases except a few sensitive ones in which five decimals were necessary. These were all rounded off to three decimals in the distributions presented in table I because it was believed that the fourth decimal might be affected by cumulative errors in such long step-by-step calculations. In table II, where initial values of  $f''$  and  $\theta'$  are listed, all four decimals are given.

An inspection of table I shows that the exact stream values of  $f'$  and  $\theta$  are not always attained. To attain these exact stream values would have entailed excessive labor without corresponding increases in the precision of  $\frac{Nu}{\sqrt{Re}}$  and  $\frac{C_{f,w}}{2} \sqrt{Re}$ . A comparison of the results between the last two trial solutions for the case of greatest deviation from exact stream values ( $T_{\infty}/T_w = 4$ ,  $Eu = 1$ , and  $f_w = -0.5$ ) was made. It was found that if  $f'$  were to approach 0.250 instead of 0.252 and  $\theta$  were to approach 1.000 instead of 0.999 at the free stream, the following approximate changes would be expected:

$\frac{Nu}{\sqrt{Re}}$  would change from 0.22522 to 0.22536

$f_w''$  would change from 0.44647 to 0.44650

$\frac{\delta^* \sqrt{Re}}{x}$  would change from 0.000 to -0.004

$\frac{\delta_i \sqrt{Re}}{x}$  would change from 1.867 to 1.856

$\frac{\delta_c \sqrt{Re}}{x}$  would change from 2.932 to 2.929

$\frac{\delta_t \sqrt{Re}}{x}$  would change from 3.233 to 3.226

In only one case is the third significant figure affected except for the value of  $\frac{\delta^* \sqrt{Re}}{x}$ , which results in an exceptional value for the particular case considered.

#### COMPARISON WITH PREVIOUS RESULTS

Specific-weight-flow, velocity, and temperature profiles obtained by both the method of reference 10 and the present method are shown in figure 1(a) for the case of maximum deviation and in figure 1(b) for the case of minimum deviation of specific-weight-flow values from stream values for the impermeable wall; the maximum deviation (fig. 1(a)) was obtained for a stream-to-wall temperature ratio  $T_{\infty}/T_w$  of 4 and an Euler number  $Eu$  of 1, whereas the minimum deviation (fig. 1(b)) resulted from a stream-to-wall temperature ratio of 2 and an Euler number

of 0.5. Figure 1(a) shows an excess of the specific-weight-flow profile of 7 percent above the free-stream value, a considerable increase in the velocity profile, and relatively little change in the temperature profile. Moreover, the new specific-weight-flow profile approaches the free-stream value with zero curvature and at a value of the nondimensional boundary-layer coordinate  $\eta$  which is now only slightly less than the corresponding values for the velocity and temperature profiles. In addition, the abrupt change in curvature of the velocity profile obtained by the method of reference 10 is eliminated and the new velocity profile is a smooth curve through the entire boundary layer.

Figure 1(b), the minimum deviation case for an impermeable wall, shows a specific-weight-flow profile excess of only about 2 percent, only a slight increase in the velocity profile, and temperature differences so slight that no change in the temperature profile can be plotted.

Much larger differences in the various profiles result for permeable walls. Figure 1(c) shows the comparison for a stream-to-wall temperature ratio of 4, an Euler number of 1, and a flow rate through the porous wall, designated by  $f_w$ , of -1, the most severe case considered. For this permeable case, the specific-weight-flow values exceeded the free-stream value by over 15 percent, and a much more pronounced increase in the velocity profile and even a considerable increase in the temperature profile resulted from the present method. In this case, as before, the abrupt change in curvature of the velocity profile obtained by the method of reference 10 no longer appears in the new solution. A comparison of figures 1(a) and 1(c) confirms the fact that thicker boundary layers result when porous cooling is considered.

Figure 2 shows a plot of the heat-transfer coefficient against the Euler number for values calculated by the present method for various stream-to-wall temperature ratios and flow rates through the porous wall designated by  $f_w = 0$ , -0.5, and -1 and for values obtained by the method of reference 10 for Euler numbers of 0.5 and 1 designated by circles for  $T_\infty/T_w = 2$  and by triangles for  $T_\infty/T_w = 4$ . The upper two curves for the impermeable wall ( $f_w = 0$ ), that is, those for  $T_\infty/T_w$  values less than unity, are presented in reference 13. The velocity values for these temperature ratios exceeded the free-stream values. No changes resulted when the two methods were used for a value of  $T_\infty/T_w \leq 1$ . It can be seen from figure 2 that the curves group themselves according to the coolant flow rates considered. Moreover, in each instance, the magnitude of the changes encountered by applying the two methods are nearly the same. Percentagewise, however, the variations increase as the cooling-air flow rate through the porous wall increases (or as the porous-flow parameter decreases).

Comparisons of the dimensionless displacement thickness of the boundary layer obtained by the two methods are shown in figure 3 for a range of Euler number, coolant flow rates through the walls of 0 and -1, and stream-to-wall temperature ratios of 2 and 4. In each case, the dimensionless displacement thickness decreased when the present method of solution was applied. These decreases result directly from the fact that the new specific-weight-flow profiles exceed the free-stream values; the integral in the definition of this boundary-layer thickness is measured by the area between the unit ordinate and the specific-weight-flow profiles. From figure 3(a), for a stream-to-wall temperature ratio of 2, it can be seen that for an Euler number of 1, the nondimensional displacement thickness decreases by about 16 percent for an impermeable wall and about 23 percent for the permeable wall. From figure 3(b), the corresponding decreases for a stream-to-wall temperature ratio of 4 are about 80 and 116 percent, respectively. For a permeable wall, figure 3(b) also shows a negative displacement thickness for large Euler numbers. From these figures it can be seen that, as the Euler number decreases, the curves representing the solutions obtained by the two methods converge.

In the calculation of the dimensionless momentum and convection thicknesses, the influence of changes in the velocity profile are present along with those of the specific-weight-flow profiles. These influences tend to counteract each other, with the net result that there are only slight differences in the momentum and convection thicknesses. For this reason, these thicknesses are not plotted. The new values are tabulated in table II; the values obtained by the method of reference 10 are available in table II of reference 10.

#### SUMMARY OF RESULTS

Under assumed conditions of constant wall temperature and small Mach numbers, solutions of the laminar-boundary-layer equations which fulfill the vanishing of the second- and higher-order derivatives of the boundary-layer stream function at the free-stream boundary were obtained for cases where large temperature changes in the boundary layer and large pressure changes in the main stream occur simultaneously. Stream-to-wall temperature ratios of 2 and 4, Euler numbers of 0.5 and 1, and porous flow rates characterized by values of the flow parameter of 0, -0.5, and -1 were considered in these calculations. Previously determined results for stream-to-wall temperature ratios less than unity resulted in velocities which exceeded the free-stream values.

The results of this analytical investigation are summarized as follows:

1. The new specific-weight-flow profiles were found to exceed the free-stream values. For an impermeable wall, a stream-to-wall temperature ratio of 2, and an Euler number of 0.5, the excess of the specific weight flow over the free-stream value was 2 percent; for a permeable wall with a coolant flow parameter of -1, a stream-to-wall temperature ratio of 4, and an Euler number of 1, the excess was 15 percent.

2. Velocity and temperature values throughout the boundary layer were larger than those previously obtained; maximum differences were found for a stream-to-wall temperature ratio of 4, an Euler number of 1, and a flow rate through the porous wall of -1.

3. Specific-weight-flow profiles approached the free-stream values with zero curvatures at values of the dimensionless boundary-layer coordinate only slightly less than the corresponding values for the velocity and temperature profiles.

4. Heat-transfer coefficients increased in value over those obtained previously; the percentage change in heat-transfer coefficients increased as the cooling-air flow rate increased.

5. Considerable reductions in the nondimensional displacement boundary-layer thicknesses resulted from application of the new method. Largest decreases were obtained for an Euler number of 1. Negative values resulted for permeable walls, large temperature ratios, and large Euler numbers. As the Euler number decreased, the solutions obtained by the two methods converged.

6. Only slight changes in the dimensionless momentum and convection thicknesses resulted when the present method of solution was used.

7. Values of the dimensionless thermal boundary-layer thickness were calculated and are included.

#### CONCLUSION

The specific-weight-flow profiles determined from analytical solutions of the laminar-boundary-layer equations, under assumed conditions of constant wall temperature and small Mach numbers, exceed the free-stream values when large pressure changes in the main stream and stream-to-wall temperature ratios greater than unity occur simultaneously.

Lewis Flight Propulsion Laboratory  
National Advisory Committee for Aeronautics  
Cleveland, Ohio, July 31, 1952



## REFERENCES

1. Brown, W. Byron: Exact Solution of the Laminar Boundary Layer Equations for a Porous Plate with Variable Fluid Properties and a Pressure Gradient in the Main Stream. Paper presented before the First U. S. National Congress of Applied Mechanics (Chicago), June 11-16, 1951.
2. Eckert, E.: Die Berechnung des Wärmeübergangs in der laminaren Grenzschicht umströmter Körper. VDI Forschungsheft 416, Bd. 13, Sept. und Okt. 1942.
3. Eckert, E. R. G., and Livingood, John N. B.: Method for Calculation of Heat Transfer in Laminar Region of Air Flow Around Cylinders of Arbitrary Cross Section (Including Large Temperature Differences and Transpiration Cooling). NACA TN 2733, 1952.
4. Falkner, V. M., and Skan, Sylvia W.: Some Approximate Solutions of the Boundary Layer Equations. R. & M. No. 1314, April 1930.
5. Eckert, E., and Drewitz, O.: The Heat Transfer to a Plate in Flow at High Speed. NACA TM 1045, 1943.
6. Tifford, Arthur N.: The Thermodynamics of the Laminar Boundary Layer of a Heated Body in a High-Speed Gas Flow Field. Jour. Aero. Sci., vol. 12, no. 2, April 1945, pp. 241-251.
7. Schuh, H.: Laminar Heat Transfer in Boundary Layers at High Velocities. Rep. and Trans. 810, British M.A.P., April 15, 1947.
8. Levy, S.: Heat Transfer to Constant Property Laminar Boundary Layer Flows with Power Function Free Stream Velocity and Wall Temperature Variation. Rep. 5, Ser. 41, Inst. Eng. Res., Univ. Calif. (Berkeley), July 25, 1951. (USAF-AMC Contract No. 33(038)-12941.)
9. Eckert, E. R. G.: Heat Transfer and Temperature Profiles in Laminar Boundary Layers on a Sweat-Cooled Wall. Tech. Rep. No. 5646, Air Materiel Command, Nov. 3, 1947.
10. Brown, W. Byron, and Donoughe, Patrick L.: Tables of Exact Laminar-Boundary-Layer Solutions When the Wall is Porous and Fluid Properties are Variable. NACA TN 2479, 1951.
11. Keenan, Joseph H., and Kaye, Joseph: Thermodynamic Properties of Air. John Wiley and Sons, Inc., 1947.
12. Scarborough, James B.: Numerical Mathematical Analysis. The Johns Hopkins Press (Baltimore), 2d ed., 1950 ch. XI.

13. Ellerbrock, Herman H., Jr.: Some NACA Investigations of Heat Transfer Characteristics of Cooled Gas-Turbine Blades. Paper presented at the General Discussion on Heat Transfer. Inst. Mech. Eng. (London) and A.S.M.E. (New York) Conference (London), Sept. 11-13, 1951.

TABLE I - VELOCITY, WEIGHT-FLOW, AND TEMPERATURE DISTRIBUTIONS  
IN LAMINAR BOUNDARY LAYER WITH VARIABLE FLUID PROPERTIES,  
PRESSURE GRADIENT IN MAIN STREAM, AND FLOW  
THROUGH POROUS WALL

$$(1) T_{\infty}/T_w = 2; Eu = 0.5; f_w = 0$$



$$\frac{\delta^* \sqrt{Re}}{x} = 0.622; \frac{\delta_1 \sqrt{Re}}{x} = 0.838; \frac{\delta_c \sqrt{Re}}{x} = 1.372; \frac{\delta_t \sqrt{Re}}{x} = 1.904$$

$\eta$	$f$	$f'$	$f''$	$f'''$	$\theta$	$\theta'$	$\theta''$	$\frac{u}{U_{\infty}}$ $Pf'$	$\frac{\rho u}{\rho_{\infty} U_{\infty}}$ $2f'$
0	0	0	0.684	-0.992	0	0.402	-0.137	0	0
.2	.012	.119	.516	-.704	.078	.377	-.114	.128	.238
.4	.046	.210	.396	-.517	.151	.356	-.101	.241	.419
.6	.095	.280	.306	-.389	.220	.336	-.093	.341	.559
.8	.156	.334	.238	-.298	.286	.318	-.089	.429	.668
1.0	.228	.376	.185	-.231	.347	.300	-.086	.506	.752
1.2	.306	.409	.144	-.181	.406	.283	-.085	.575	.817
1.4	.391	.434	.112	-.142	.461	.266	-.084	.634	.869
1.6	.480	.454	.087	-.113	.512	.250	-.083	.687	.908
1.8	.572	.469	.067	-.089	.561	.233	-.082	.733	.939
2.0	.667	.481	.051	-.071	.606	.217	-.081	.773	.962
2.2	.764	.490	.038	-.056	.648	.201	-.079	.807	.980
2.4	.863	.496	.028	-.044	.686	.186	-.077	.837	.993
2.6	.963	.501	.020	-.035	.722	.170	-.075	.863	1.003
2.8	1.063	.505	.014	-.027	.754	.156	-.072	.885	1.009
3.2	1.266	.508	.005	-.016	.811	.128	-.065	.921	1.017
3.6	1.470	.510	0	-.009	.857	.103	-.058	.946	1.019
4.0	1.673	.509	-.002	-.004	.894	.082	-.050	.964	1.018
4.4	1.877	.508	-.003	-.001	.923	.063	-.042	.977	1.016
4.8	2.080	.507	-.004	0	.946	.048	-.035	.986	1.013
5.2	2.282	.505	-.003	.001	.962	.035	-.028	.991	1.010
5.6	2.484	.504	-.003	.001	.974	.026	-.022	.995	1.008
6.0	2.685	.503	-.002	.002	.983	.018	-.016	.997	1.006
6.4	2.886	.502	-.002	.001	.989	.012	-.012	.999	1.005
6.8	3.087	.502	-.001	.001	.993	.008	-.009	1.000	1.004
7.2	3.288	.501	-.001	.001	.996	.005	-.006	1.001	1.003
7.6	3.488	.501	0	.001	.998	.003	-.004	1.001	1.002
8.0	3.689	.501	0	0	.999	.002	-.003	1.002	1.002
8.4	3.889	.501	0	0	.999	.001	-.002	1.002	1.002
8.8	4.090				1.000	.001	-.001	1.002	
9.2	4.290				1.000	0	-.001	1.002	
9.6	4.490				1.000	0	0	1.002	
10.0	4.691				1.000	0	0	1.002	

TABLE I - VELOCITY, WEIGHT-FLOW, AND TEMPERATURE DISTRIBUTIONS  
IN LAMINAR BOUNDARY LAYER WITH VARIABLE FLUID PROPERTIES,  
PRESSURE GRADIENT IN MAIN STREAM, AND FLOW  
THROUGH POROUS WALL - Continued

(2)  $T_\infty/T_w = 2$ ;  $Eu = 1$ ;  $f_w = 0$



$\frac{\delta^* \sqrt{Re}}{x} = 0.433$ ;  $\frac{\delta_i \sqrt{Re}}{x} = 0.693$ ;  $\frac{\delta_c \sqrt{Re}}{x} = 1.215$ ;  $\frac{\delta_t \sqrt{Re}}{x} = 1.611$

$\eta$	$f$	$f'$	$f''$	$f'''$	$\theta$	$\theta'$	$\theta''$	$\frac{u}{U_\infty}$ $Pf'$	$\frac{\rho u}{\rho_\infty U_\infty}$ $2f'$
0	0	0	0.909	-1.668	0	0.476	-0.193	0	0
.1	.004	.083	.758	-1.352	.047	.458	-.172	.087	.167
.2	.016	.153	.636	-1.108	.092	.441	-.156	.167	.306
.3	.034	.211	.535	-.918	.135	.426	-.146	.240	.422
.4	.058	.260	.451	-.765	.177	.412	-.138	.306	.521
.5	.086	.302	.381	-.642	.218	.399	-.132	.367	.604
.6	.118	.337	.322	-.541	.257	.386	-.128	.423	.674
.7	.154	.367	.272	-.456	.295	.373	-.125	.475	.733
.8	.192	.392	.230	-.387	.332	.361	-.123	.522	.783
.9	.232	.413	.195	-.329	.367	.349	-.122	.564	.826
1.0	.274	.431	.164	-.280	.401	.337	-.120	.604	.862
1.1	.318	.446	.138	-.239	.434	.325	-.119	.640	.892
1.2	.363	.459	.116	-.204	.466	.313	-.118	.672	.917
1.4	.457	.478	.081	-.149	.526	.289	-.117	.730	.956
1.6	.554	.492	.056	-.109	.582	.266	-.114	.778	.984
1.8	.653	.501	.037	-.079	.633	.243	-.111	.818	1.002
2.0	.754	.507	.023	-.058	.679	.221	-.108	.851	1.014
2.2	.856	.511	.014	-.041	.721	.200	-.104	.879	1.021
2.4	.958	.513	.006	-.029	.759	.180	-.099	.902	1.025
2.6	1.061	.514	.002	-.020	.793	.161	-.093	.921	1.027
2.8	1.164	.514	-.002	-.013	.824	.143	-.088	.937	1.027
3.0	1.266	.513	-.004	-.008	.851	.126	-.082	.949	1.026
3.2	1.369	.512	-.005	-.005	.874	.110	-.075	.960	1.024
3.6	1.573	.510	-.006	0	.913	.083	-.062	.975	1.019
4.0	1.777	.507	-.006	.002	.941	.060	-.050	.985	1.015
4.4	1.979	.505	-.005	.003	.961	.043	-.039	.991	1.010
4.8	2.181	.504	-.004	.003	.976	.029	-.029	.995	1.007
5.2	2.382	.502	-.003	.002	.985	.019	-.021	.997	1.005
5.6	2.583	.501	-.002	.002	.992	.012	-.014	.999	1.003
6.0	2.783	.501	-.001	.001	.996	.008	-.010	.999	1.002
6.4	2.984	.500	-.001	.001	.998	.005	-.006	1.000	1.001
6.8	3.184	.500	0	.001	1.000	.003	-.004	1.000	1.000
7.2	3.384	.500	0	0	1.000	.001	-.002	1.000	1.000
7.6	3.584	.500	0	0	1.001	.001	-.001	1.000	1.000
8.0	3.784	.500	0	0	1.001	0	-.001	1.000	.999
8.4	3.983	.500	0	0	1.001	0	0	1.000	.999
8.8	4.183				1.001	0	0	1.000	

TABLE I - VELOCITY, WEIGHT-FLOW, AND TEMPERATURE DISTRIBUTIONS  
IN LAMINAR BOUNDARY LAYER WITH VARIABLE FLUID PROPERTIES,  
PRESSURE GRADIENT IN MAIN STREAM, AND FLOW  
THROUGH POROUS WALL - Continued

(3)  $T_\infty/T_w = 2$ ;  $Eu = 0.5$ ;  $f_w = -0.5$



$$\frac{\delta^* \sqrt{Re}}{x} = 0.772; \frac{\delta_1 \sqrt{Re}}{x} = 1.044; \frac{\delta_c \sqrt{Re}}{x} = 1.771; \frac{\delta_t \sqrt{Re}}{x} = 2.476$$

$\eta$	$f$	$f'$	$f''$	$f'''$	$\theta$	$\theta'$	$\theta''$	$\frac{u}{U_\infty}$ $Pf'$	$\frac{\rho u}{\rho_\infty U_\infty}$ $2f'$
0	-0.500	0	0.477	-0.368	0	0.230	0.015	0	0
.2	-.491	.088	.408	-.325	.046	.233	.014	.093	.177
.4	-.466	.164	.347	-.286	.093	.236	.011	.179	.327
.6	-.426	.228	.293	-.250	.141	.238	.007	.260	.455
.8	-.375	.282	.247	-.218	.188	.239	.001	.335	.563
1.0	-.314	.327	.206	-.188	.236	.238	-.005	.404	.653
1.2	-.245	.364	.171	-.162	.284	.237	-.011	.468	.729
1.4	-.169	.396	.141	-.138	.331	.234	-.018	.526	.791
1.6	-.087	.421	.116	-.117	.377	.230	-.024	.580	.842
1.8	-.001	.442	.094	-.099	.423	.224	-.030	.629	.884
2.0	.089	.459	.076	-.084	.467	.218	-.035	.673	.918
2.4	.278	.483	.048	-.058	.551	.202	-.044	.750	.967
2.8	.475	.498	.028	-.040	.628	.183	-.050	.811	.997
3.2	.676	.507	.015	-.026	.697	.162	-.054	.860	1.014
3.6	.880	.511	.007	-.017	.757	.140	-.054	.898	1.022
4.0	1.084	.513	.001	-.010	.809	.119	-.052	.927	1.025
4.4	1.289	.512	-.002	-.006	.852	.098	-.049	.949	1.025
4.8	1.494	.511	-.003	-.002	.888	.080	-.044	.965	1.023
5.2	1.698	.510	-.004	0	.917	.063	-.039	.977	1.020
5.6	1.902	.508	-.004	.001	.939	.049	-.033	.985	1.016
6.0	2.105	.507	-.004	.001	.956	.037	-.027	.991	1.013
6.4	2.307	.505	-.003	.002	.969	.027	-.022	.995	1.011
6.8	2.509	.504	-.002	.002	.978	.020	-.017	.998	1.009
7.2	2.711	.504	-.002	.002	.985	.014	-.012	1.000	1.007
7.6	2.912	.503	-.001	.001	.990	.010	-.009	1.001	1.006
8.0	3.113	.503	-.001	.001	.993	.006	-.007	1.002	1.005
8.4	3.314	.502	0	.001	.995	.004	-.005	1.002	1.005
8.8	3.515	.502	0	0	.997	.003	-.003	1.003	1.005
9.2	3.714	.502	0	0	.997	.002	-.002	1.003	1.005
9.6	3.915				.998	.001	-.001	1.004	
10.0	4.116				.998	.001	-.001	1.004	
10.4	4.317				.999	0	-.001	1.004	
10.8	4.518				.999	0	0	1.004	
11.2	4.719				.999	0	0	1.004	

TABLE I - VELOCITY, WEIGHT-FLOW, AND TEMPERATURE DISTRIBUTIONS  
IN LAMINAR BOUNDARY LAYER WITH VARIABLE FLUID PROPERTIES,  
PRESSURE GRADIENT IN MAIN STREAM, AND FLOW  
THROUGH POROUS WALL - Continued

(4)  $T_{\infty}/T_w = 2$ ;  $Eu = 1.0$ ;  $f_w = -0.5$



$\frac{\delta^* \sqrt{Re}}{x} = 0.507$ ;  $\frac{\delta_1 \sqrt{Re}}{x} = 0.880$ ;  $\frac{\delta_c \sqrt{Re}}{x} = 1.638$ ;  $\frac{\delta_t \sqrt{Re}}{x} = 2.151$

$\eta$	$f$	$f'$	$f''$	$f'''$	$\theta$	$\theta'$	$\theta''$	$\frac{u}{U_{\infty}}$ $\frac{Pf'}{Pf'}$	$\frac{\rho u}{\rho_{\infty} U_{\infty}}$ $\frac{2f'}{2f'}$
0	-0.500	0	0.642	-0.623	0	0.256	0.034	0	0
.2	-.488	.116	.524	-.547	.052	.263	.031	.122	.233
.4	-.455	.211	.423	-.470	.105	.268	.025	.233	.422
.6	-.405	.286	.336	-.396	.159	.272	.016	.332	.573
.8	-.342	.346	.264	-.328	.214	.274	.005	.420	.693
1.0	-.267	.393	.205	-.267	.268	.274	-.006	.498	.786
1.2	-.185	.429	.156	-.216	.323	.271	-.018	.567	.858
1.4	-.096	.456	.118	-.172	.377	.266	-.029	.628	.912
1.6	-.003	.477	.087	-.136	.429	.259	-.040	.681	.953
1.8	.094	.492	.063	-.106	.480	.251	-.049	.728	.983
2.0	.193	.502	.044	-.082	.530	.240	-.057	.768	1.005
2.2	.295	.510	.030	-.063	.576	.228	-.063	.803	1.019
2.4	.397	.514	.019	-.048	.621	.215	-.068	.834	1.029
2.8	.604	.519	.005	-.026	.701	.187	-.073	.883	1.038
3.2	.812	.519	-.003	-.013	.770	.157	-.073	.919	1.039
3.6	1.019	.517	-.006	-.005	.827	.129	-.069	.945	1.035
4.0	1.226	.514	-.007	-.001	.873	.102	-.063	.964	1.029
4.4	1.431	.512	-.007	.002	.909	.079	-.054	.977	1.023
4.8	1.635	.509	-.006	.003	.937	.059	-.045	.986	1.018
5.2	1.838	.507	-.005	.003	.957	.043	-.036	.992	1.013
5.6	2.040	.505	-.004	.003	.971	.030	-.028	.995	1.010
6.0	2.242	.504	-.003	.003	.981	.020	-.021	.998	1.007
6.4	2.443	.503	-.002	.002	.988	.013	-.015	1.000	1.006
6.8	2.644	.502	-.001	.002	.992	.009	-.010	1.001	1.004
7.2	2.845	.502	0	.001	.995	.005	-.006	1.001	1.004
7.6	3.046	.502	0	.001	.997	.003	-.005	1.002	1.003
8.0	3.247	.502	0	0	.998	.002	-.002	1.002	1.003
8.4	3.447				.998	.001	-.002	1.002	
8.8	3.648				.999	.001	-.001	1.003	
9.2	3.849				.999	0	0	1.003	
9.6	4.049				.999	0	0	1.003	

TABLE I - VELOCITY, WEIGHT-FLOW, AND TEMPERATURE DISTRIBUTIONS  
IN LAMINAR BOUNDARY LAYER WITH VARIABLE FLUID PROPERTIES,  
PRESSURE GRADIENT IN MAIN STREAM, AND FLOW  
THROUGH POROUS WALL - Continued

$$(5) T_{\infty}/T_w = 2; Eu = 0.5; f_w = -1.0$$



$$\frac{\delta^* \sqrt{Re}}{x} = 0.965; \frac{\delta_1 \sqrt{Re}}{x} = 1.310; \frac{\delta_c \sqrt{Re}}{x} = 2.298; \frac{\delta_t \sqrt{Re}}{x} = 3.236$$

$\eta$	$f$	$f'$	$f''$	$f'''$	$\theta$	$\theta'$	$\theta''$	$\frac{u}{U_{\infty}}$ $Pf'$	$\frac{\rho u}{\rho_{\infty} U_{\infty}}$ $2f'$
0	-1.000	0	0.323	-0.100	0	0.106	0.046	0	0
.2	-.994	.062	.302	-.108	.022	.116	.048	.064	.125
.4	-.975	.121	.280	-.113	.046	.125	.050	.126	.241
.6	-.946	.174	.257	-.117	.072	.135	.050	.187	.349
.8	-.906	.223	.233	-.118	.100	.145	.049	.246	.447
1.0	-.857	.268	.210	-.117	.130	.155	.046	.303	.535
1.2	-.799	.307	.187	-.114	.162	.164	.043	.357	.615
1.4	-.734	.342	.164	-.109	.196	.172	.038	.409	.685
1.6	-.662	.373	.143	-.102	.231	.179	.032	.459	.747
1.8	-.585	.400	.124	-.094	.267	.185	.026	.507	.800
2.0	-.503	.423	.106	-.086	.304	.189	.019	.552	.846
2.2	-.416	.442	.089	-.078	.343	.192	.011	.594	.885
2.4	-.326	.459	.074	-.069	.381	.194	.004	.633	.917
2.8	-.137	.483	.050	-.053	.459	.192	-.011	.705	.966
3.2	.060	.499	.032	-.039	.534	.185	-.023	.766	.999
3.6	.261	.509	.018	-.028	.606	.174	-.033	.818	1.018
4.0	.466	.514	.009	-.019	.673	.159	-.041	.861	1.029
4.4	.672	.517	.002	-.012	.733	.142	-.045	.895	1.033
4.8	.879	.517	-.001	-.008	.787	.124	-.046	.923	1.034
5.2	1.086	.516	-.004	-.004	.832	.105	-.045	.945	1.032
5.6	1.292	.514	-.005	-.002	.871	.088	-.043	.962	1.028
6.0	1.497	.512	-.005	0	.903	.071	-.039	.974	1.024
6.4	1.701	.510	-.005	.001	.928	.057	-.034	.984	1.020
7.2	2.108	.506	-.004	.002	.964	.033	-.024	.994	1.013
8.0	2.512	.504	-.002	.002	.984	.018	-.015	1.000	1.008
8.8	2.914	.502	-.001	.001	.994	.009	-.008	1.002	1.005
9.6	3.316	.502	0	.001	.999	.004	-.004	1.003	1.004
10.4	3.717	.502	0	.001	1.001	.001	-.002	1.004	1.003
11.2	4.119				1.002	0	-.001	1.004	
12.0	4.520				1.002	0	0	1.004	

TABLE I - VELOCITY, WEIGHT-FLOW, AND TEMPERATURE DISTRIBUTIONS  
IN LAMINAR BOUNDARY LAYER WITH VARIABLE FLUID PROPERTIES,  
PRESSURE GRADIENT IN MAIN STREAM, AND FLOW  
THROUGH POROUS WALL - Continued

$$(6) T_{\infty}/T_w = 2; Eu = 1; f_w = -1.0$$



$$\frac{\delta^* \sqrt{Re}}{x} = 0.608; \frac{\delta_i \sqrt{Re}}{x} = 1.148; \frac{\delta_c \sqrt{Re}}{x} = 2.228; \frac{\delta_t \sqrt{Re}}{x} = 2.891$$

$\eta$	$f$	$f'$	$f''$	$f'''$	$\theta$	$\theta'$	$\theta''$	$\frac{u}{U_{\infty}}$ $Pf'$	$\frac{\rho u}{\rho_{\infty} U_{\infty}}$ $2f'$
0	-1.000	0	0.445	-0.182	0	0.105	0.064	0	0
.2	-.991	.085	.406	-.202	.022	.119	.069	.087	.170
.4	-.966	.162	.364	-.214	.048	.133	.073	.170	.324
.6	-.927	.231	.321	-.218	.076	.148	.074	.248	.462
.8	-.875	.291	.278	-.215	.107	.162	.073	.322	.581
1.0	-.811	.342	.236	-.204	.140	.176	.069	.390	.684
1.2	-.739	.385	.196	-.189	.177	.190	.062	.453	.770
1.4	-.658	.421	.160	-.170	.216	.201	.053	.512	.841
1.6	-.571	.450	.128	-.150	.257	.211	.042	.565	.899
1.8	-.478	.472	.100	-.129	.300	.218	.030	.614	.945
2.0	-.382	.490	.077	-.108	.345	.223	.018	.659	.980
2.4	-.181	.513	.041	-.073	.434	.225	-.007	.736	1.026
2.8	.026	.524	.017	-.046	.523	.217	-.029	.798	1.048
3.2	.237	.528	.003	-.027	.607	.202	-.046	.849	1.056
3.6	.448	.528	-.005	-.014	.684	.181	-.057	.888	1.055
4.0	.659	.525	-.009	-.006	.752	.157	-.062	.919	1.050
4.4	.868	.521	-.010	-.001	.810	.132	-.062	.943	1.042
4.8	1.076	.517	-.010	.002	.858	.108	-.059	.960	1.034
5.2	1.282	.513	-.009	.003	.896	.085	-.053	.973	1.026
5.6	1.486	.510	-.008	.004	.926	.065	-.046	.982	1.020
6.0	1.690	.507	-.006	.004	.949	.048	-.038	.988	1.014
6.4	1.892	.505	-.005	.003	.965	.035	-.030	.992	1.010
6.8	2.094	.503	-.004	.003	.977	.024	-.023	.995	1.007
7.2	2.295	.502	-.003	.002	.985	.016	-.017	.997	1.004
7.6	2.496	.501	-.002	.002	.990	.011	-.012	.998	1.002
8.0	2.696	.501	-.001	.001	.994	.007	-.008	.998	1.001
8.4	2.896	.500	-.001	.001	.996	.004	-.005	.998	1.000
8.8	3.096	.500	-.001	.001	.997	.002	-.003	.998	1.000
9.2	3.296	.500	0	0	.998	.001	-.002	.998	.999
9.6	3.496				.998	.001	-.001	.999	
10.0	3.696				.999	0	-.001	.999	
10.4	3.896				.999	0	0	.999	
10.8	4.096				.999	0	0	.999	



TABLE I - VELOCITY, WEIGHT-FLOW, AND TEMPERATURE DISTRIBUTIONS  
IN LAMINAR BOUNDARY LAYER WITH VARIABLE FLUID PROPERTIES,  
PRESSURE GRADIENT IN MAIN STREAM, AND FLOW  
THROUGH POROUS WALL - Continued

$$(7) T_{\infty}/T_w = 4; Eu = 0.5; f_w = 0$$



$$\frac{\delta^* \sqrt{Re}}{x} = 0.272; \frac{\delta_1 \sqrt{Re}}{x} = 1.676; \frac{\delta_c \sqrt{Re}}{x} = 2.399; \frac{\delta_t \sqrt{Re}}{x} = 2.790$$

$\eta$	$f$	$f'$	$f''$	$f'''$	$\theta$	$\theta'$	$\theta''$	$\frac{u}{U_{\infty}}$ $Pf'$	$\frac{\rho u}{\rho_{\infty} U_{\infty}}$ $4f'$
0	0	0	0.554	-1.893	0	0.394	-0.396	0	0
.1	.002	.047	.406	-1.160	.038	.360	-.297	.053	.190
.2	.009	.083	.312	-.773	.072	.333	-.234	.101	.332
.3	.019	.111	.248	-.545	.104	.312	-.192	.146	.444
.4	.031	.133	.201	-.400	.135	.295	-.161	.187	.533
.5	.045	.151	.166	-.304	.164	.280	-.139	.226	.606
.6	.061	.167	.139	-.237	.191	.267	-.122	.262	.666
.7	.078	.179	.118	-.189	.217	.255	-.108	.296	.718
.8	.097	.190	.100	-.153	.242	.245	-.097	.328	.761
.9	.116	.200	.086	-.126	.266	.236	-.089	.359	.798
1.0	.137	.208	.075	-.105	.289	.227	-.081	.388	.831
1.1	.158	.215	.065	-.089	.312	.220	-.075	.415	.859
1.2	.180	.221	.057	-.076	.333	.212	-.070	.442	.883
1.3	.202	.226	.050	-.065	.354	.206	-.066	.466	.904
1.4	.225	.231	.044	-.056	.374	.199	-.062	.490	.923
1.6	.272	.239	.034	-.042	.413	.187	-.056	.534	.954
1.8	.320	.245	.027	-.033	.449	.177	-.051	.575	.979
2.0	.370	.249	.021	-.026	.484	.167	-.047	.611	.998
2.2	.420	.253	.016	-.020	.516	.158	-.044	.645	1.012
2.4	.471	.256	.013	-.016	.547	.150	-.041	.676	1.024
2.6	.522	.258	.010	-.013	.576	.142	-.039	.705	1.033
2.8	.574	.260	.007	-.011	.604	.134	-.037	.731	1.040
3.0	.626	.261	.005	-.009	.630	.127	-.035	.755	1.044
3.2	.679	.262	.004	-.007	.655	.120	-.033	.777	1.048
3.4	.731	.263	.002	-.006	.678	.113	-.032	.797	1.050
3.6	.784	.263	.001	-.005	.700	.107	-.030	.815	1.052
3.8	.836	.263	0	-.004	.721	.101	-.029	.832	1.053
4.0	.889	.263	0	-.003	.740	.096	-.028	.848	1.053
4.4	.994	.263	-.001	-.002	.777	.085	-.026	.875	1.051
4.8	1.099	.262	-.002	-.001	.809	.075	-.023	.898	1.048
5.2	1.204	.261	-.002	-.001	.837	.066	-.021	.917	1.045
5.6	1.308	.260	-.003	0	.862	.058	-.020	.933	1.041
6.0	1.412	.259	-.003	0	.883	.051	-.018	.946	1.036
6.4	1.515	.258	-.003	0	.902	.044	-.016	.956	1.032
6.8	1.618	.257	-.002	0	.919	.038	-.014	.965	1.028
7.2	1.721	.256	-.002	0	.933	.032	-.013	.972	1.024
7.6	1.823	.255	-.002	0	.945	.028	-.011	.978	1.020
8.0	1.925	.254	-.002	0	.955	.023	-.010	.983	1.017
8.8	2.128	.253	-.002	0	.971	.016	-.008	.989	1.012
9.6	2.330	.252	-.001	0	.981	.011	-.006	.994	1.008
10.4	2.531	.251	-.001	0	.989	.007	-.004	.996	1.004
11.2	2.732	.250	-.001	0	.993	.005	-.003	.997	1.002
12.0	2.932	.250	0	0	.997	.003	-.002	.998	1.000
12.8	2.132	.250			.999	.002	-.001	.998	.999
13.6	3.332	.250			1.000	.001	-.001	.998	.998
14.4	3.531	.250			1.000	.001	0	.998	.998
15.2	3.731	.249			1.001	0	0	.998	.998
16.0	3.930				1.001	0	0	.998	

TABLE I - VELOCITY, WEIGHT-FLOW, AND TEMPERATURE DISTRIBUTIONS  
IN LAMINAR BOUNDARY LAYER WITH VARIABLE FLUID PROPERTIES,  
PRESSURE GRADIENT IN MAIN STREAM, AND FLOW  
THROUGH POROUS WALL - Continued

$$(8) T_{\infty}/T_w = 4; Eu = 1; f_w = 0$$



$$\frac{\delta^* \sqrt{Re}}{x} = 0.081; \frac{\delta_1 \sqrt{Re}}{x} = 1.403; \frac{\delta_c \sqrt{Re}}{x} = 2.113; \frac{\delta_t \sqrt{Re}}{x} = 2.370$$

$\eta$	$f$	$f'$	$f''$	$f'''$	$\theta$	$\theta'$	$\theta''$	$\frac{u}{U_{\infty}}$ $Pr'$	$\frac{\rho u}{\rho_{\infty} U_{\infty}}$ $4f'$
0	0	0	0.722	-2.976	0	0.466	-0.554	0	0
.05	.001	.033	.594	-2.202	.023	.441	-.464	.035	.131
.10	.003	.060	.498	-1.683	.044	.419	-.397	.068	.240
.15	.007	.083	.423	-1.320	.065	.401	-.345	.099	.332
.20	.011	.102	.364	-1.058	.084	.385	-.304	.128	.410
.25	.017	.120	.316	-.863	.103	.370	-.271	.156	.478
.30	.023	.134	.277	-.715	.121	.357	-.244	.183	.537
.4	.038	.159	.216	-.508	.156	.335	-.202	.233	.635
.5	.055	.178	.173	-.375	.188	.317	-.172	.279	.713
.6	.074	.194	.140	-.285	.219	.301	-.150	.321	.775
.7	.094	.206	.115	-.222	.249	.286	-.133	.361	.826
.8	.115	.217	.095	-.176	.277	.274	-.119	.397	.868
.9	.137	.226	.079	-.142	.303	.262	-.108	.431	.903
1.0	.160	.233	.066	-.116	.329	.252	-.099	.463	.932
1.1	.184	.239	.056	-.096	.354	.242	-.092	.493	.956
1.2	.208	.244	.047	-.080	.378	.234	-.086	.521	.976
1.4	.257	.252	.033	-.057	.423	.217	-.076	.572	1.008
1.6	.308	.258	.024	-.041	.465	.203	-.068	.617	1.030
1.8	.360	.262	.016	-.031	.504	.190	-.063	.657	1.046
2.0	.413	.264	.011	-.023	.541	.178	-.058	.693	1.057
2.2	.466	.266	.007	-.017	.575	.167	-.054	.725	1.064
2.4	.519	.267	.004	-.013	.608	.156	-.051	.754	1.069
2.8	.626	.268	0	-.007	.666	.137	-.045	.804	1.072
3.2	.734	.268	-.002	-.004	.718	.120	-.041	.844	1.070
3.6	.840	.266	-.004	-.002	.763	.105	-.037	.876	1.065
4.0	.946	.265	-.004	-.001	.802	.091	-.033	.901	1.059
4.4	1.052	.263	-.004	0	.836	.078	-.030	.922	1.052
4.8	1.157	.261	-.004	0	.865	.067	-.027	.939	1.045
5.2	1.261	.260	-.004	.001	.889	.057	-.024	.953	1.039
5.6	1.365	.258	-.004	.001	.910	.048	-.021	.963	1.032
6.4	1.570	.256	-.003	.001	.943	.033	-.016	.978	1.022
7.2	1.774	.254	-.002	.001	.965	.022	-.012	.988	1.015
8.0	1.976	.252	-.001	.001	.979	.014	-.008	.994	1.010
8.8	2.178	.252	-.001	0	.988	.009	-.005	.997	1.006
9.6	2.379	.251	-.001	0	.994	.005	-.003	.999	1.004
10.4	2.579	.250	0	0	.997	.003	-.002	.999	1.002
11.2	2.780	.250	0	0	.999	.002	-.001	1.000	1.001
12.0	2.980	.250	0	0	1.000	.001	-.001	1.000	1.000
12.8	3.180	.250	0	0	1.000	0	0	1.000	1.000
13.6	3.380				1.001	0	0	1.001	
14.4	3.580				1.001	0	0	1.001	

TABLE I - VELOCITY, WEIGHT-FLOW, AND TEMPERATURE DISTRIBUTIONS  
IN LAMINAR BOUNDARY LAYER WITH VARIABLE FLUID PROPERTIES,  
PRESSURE GRADIENT IN MAIN STREAM, AND FLOW  
THROUGH POROUS WALL - Continued

$$(9) T_{\infty}/T_w = 4; Eu = 0.5; f_w = -0.5$$



$$\frac{\delta^* \sqrt{Re}}{x} = 0.318; \frac{\delta_1 \sqrt{Re}}{x} = 2.155; \frac{\delta_c \sqrt{Re}}{x} = 3.142; \frac{\delta_t \sqrt{Re}}{x} = 3.670$$

$\eta$	$f$	$f'$	$f''$	$f'''$	$\theta$	$\theta'$	$\theta''$	$\frac{u}{U_{\infty}}$ $Pf'$	$\frac{pu}{\rho_{\infty} U_{\infty}}$ $4f'$
0	-0.500	0	0.345	-0.579	0	0.209	-0.056	0	0
.2	-.494	.059	.252	-.371	.041	.199	-.042	.066	.236
.4	-.477	.103	.191	-.255	.080	.191	-.034	.128	.412
.6	-.453	.137	.148	-.183	.117	.185	-.028	.185	.546
.8	-.423	.163	.116	-.135	.154	.180	-.025	.238	.652
1.0	-.389	.184	.092	-.103	.189	.175	-.023	.288	.735
1.2	-.350	.200	.074	-.080	.224	.170	-.022	.335	.801
1.4	-.309	.214	.060	-.063	.258	.166	-.021	.379	.855
1.6	-.265	.225	.049	-.050	.290	.162	-.021	.420	.898
1.8	-.219	.233	.040	-.041	.322	.158	-.021	.459	.934
2.0	-.172	.241	.032	-.033	.354	.153	-.021	.496	.962
2.2	-.123	.246	.026	-.027	.384	.149	-.021	.530	.986
2.4	-.073	.251	.021	-.022	.413	.145	-.021	.563	1.005
2.8	.029	.258	.014	-.016	.470	.137	-.021	.622	1.032
3.2	.133	.262	.008	-.011	.523	.128	-.021	.674	1.050
3.6	.239	.265	.005	-.008	.572	.120	-.021	.720	1.060
4.0	.345	.266	.002	-.005	.618	.111	-.021	.761	1.066
4.4	.452	.267	0	-.004	.661	.103	-.021	.797	1.068
4.8	.559	.267	-.001	-.003	.701	.095	-.021	.828	1.067
5.2	.665	.266	-.002	-.002	.737	.086	-.020	.855	1.065
5.6	.772	.265	-.002	-.001	.770	.079	-.019	.878	1.062
6.0	.878	.264	-.003	-.001	.800	.071	-.018	.899	1.058
6.4	.983	.263	-.003	0	.827	.064	-.017	.916	1.053
7.2	1.193	.261	-.003	0	.873	.051	-.015	.943	1.043
8.0	1.400	.258	-.003	0	.909	.039	-.013	.963	1.034
8.8	1.606	.256	-.002	.001	.936	.030	-.011	.977	1.026
9.6	1.811	.255	-.002	.001	.956	.022	-.009	.986	1.019
10.4	2.014	.253	-.002	.001	.971	.015	-.007	.992	1.014
11.2	2.216	.252	-.001	0	.981	.011	-.005	.996	1.010
12.0	2.418	.252	-.001	0	.988	.007	-.004	.998	1.006
12.8	2.619	.251	-.001	0	.993	.005	-.003	.999	1.004
13.6	2.820	.251	0	0	.996	.003	-.002	1.000	1.002
14.4	3.020	.250	0	0	.998	.002	-.001	1.000	1.002
15.2	3.220	.250	0	0	1.000	.001	-.001	1.001	1.001
16.0	3.420	.250	0	0	1.000	.001	0	1.001	1.001
16.8	3.621				1.001	0	0	1.001	
17.6	3.821				1.001	0	0	1.001	

TABLE I - VELOCITY, WEIGHT-FLOW, AND TEMPERATURE DISTRIBUTIONS  
IN LAMINAR BOUNDARY LAYER WITH VARIABLE FLUID PROPERTIES,  
PRESSURE GRADIENT IN MAIN STREAM, AND FLOW  
THROUGH POROUS WALL - Continued

$$(10) T_{\infty}/T_w = 4; Eu = 1; f_w = -0.5$$



$$\frac{\delta^* \sqrt{Re}}{x} = 0.000; \frac{\delta_1 \sqrt{Re}}{x} = 1.867; \frac{\delta_c \sqrt{Re}}{x} = 2.932; \frac{\delta_t \sqrt{Re}}{x} = 3.233$$

$\eta$	$f$	$f'$	$f''$	$f'''$	$\theta$	$\theta'$	$\theta''$	$\frac{u}{U_{\infty} Pf'}$	$\frac{\rho u}{\rho_{\infty} U_{\infty} 4f'}$
0	-0.500	0	0.446	-0.841	0	0.225	-0.051	0	0
.1	-.498	.041	.372	-.662	.022	.221	-.043	.044	.163
.2	-.492	.075	.313	-.531	.044	.217	-.037	.085	.300
.3	-.483	.104	.265	-.432	.066	.213	-.033	.124	.415
.4	-.472	.128	.225	-.356	.087	.210	-.030	.161	.512
.5	-.458	.149	.193	-.297	.108	.207	-.028	.197	.596
.6	-.442	.167	.166	-.249	.128	.204	-.026	.231	.668
.7	-.424	.182	.143	-.210	.149	.202	-.025	.264	.729
.8	-.405	.196	.123	-.179	.169	.199	-.024	.295	.782
1.0	-.364	.217	.092	-.132	.208	.195	-.023	.352	.868
1.2	-.319	.233	.070	-.099	.246	.190	-.023	.405	.932
1.4	-.271	.245	.052	-.075	.284	.185	-.024	.454	.981
1.6	-.221	.254	.039	-.057	.321	.180	-.024	.499	1.017
1.8	-.169	.261	.029	-.044	.356	.175	-.025	.540	1.044
2.0	-.117	.266	.021	-.034	.391	.170	-.026	.578	1.064
2.2	-.063	.270	.015	-.027	.424	.165	-.026	.613	1.079
2.4	-.009	.272	.010	-.021	.457	.160	-.027	.645	1.089
2.8	.101	.275	.004	-.013	.519	.149	-.028	.703	1.100
3.2	.211	.276	0	-.008	.576	.138	-.028	.752	1.102
3.6	.321	.275	-.003	-.005	.629	.126	-.028	.793	1.099
4.0	.430	.273	-.004	-.003	.677	.115	-.028	.829	1.094
4.4	.540	.272	-.005	-.001	.721	.104	-.027	.859	1.086
4.8	.648	.270	-.005	0	.761	.094	-.026	.884	1.078
5.6	.862	.265	-.005	.001	.827	.074	-.024	.924	1.062
6.4	1.072	.262	-.004	.001	.879	.056	-.020	.952	1.047
7.2	1.280	.259	-.004	.001	.918	.041	-.017	.971	1.034
8.0	1.486	.256	-.003	.001	.946	.029	-.013	.983	1.025
8.8	1.690	.254	-.002	.001	.965	.020	-.010	.991	1.018
9.6	1.893	.253	-.001	.001	.979	.013	-.007	.996	1.012
10.4	2.096	.252	-.001	0	.987	.009	-.005	1.000	1.009
11.2	2.297	.252	0	0	.993	.005	-.004	1.002	1.007
12.0	2.499	.252	0	0	.996	.003	-.002	1.003	1.006
12.8	2.700	.252	0	0	.998	.002	-.001	1.005	1.006
13.6	2.901				.999	.001	-.001	1.005	
14.4	3.102				.999	0	-.001	1.006	
15.2	3.304				.999	0	0	1.006	
16.0	3.505				.999	0	0	1.006	

TABLE I - VELOCITY, WEIGHT-FLOW, AND TEMPERATURE DISTRIBUTIONS  
IN LAMINAR BOUNDARY LAYER WITH VARIABLE FLUID PROPERTIES,  
PRESSURE GRADIENT IN MAIN STREAM, AND FLOW  
THROUGH POROUS WALL - Continued

$$(11) T_{\infty}/T_w = 4; Eu = 0.5; f_w = -1.0$$



$$\frac{\delta^* \sqrt{Re}}{x} = 0.402; \frac{\delta_1 \sqrt{Re}}{x} = 2.882; \frac{\delta_c \sqrt{Re}}{x} = 4.255; \frac{\delta_t \sqrt{Re}}{x} = 4.954$$

$\eta$	$f$	$f'$	$f''$	$f'''$	$\theta$	$\theta'$	$\theta''$	$\frac{u}{U_{\infty}}$ $\frac{Pf'}{Pf'}$	$\frac{\rho u}{\rho_{\infty} U_{\infty}}$ $\frac{4f'}{4f'}$
0	-1.000	0	0.196	-0.102	0	0.078	0.025	0	0
.4	-.985	.070	.157	-.093	.033	.088	.025	.077	.282
.8	-.946	.126	.122	-.081	.070	.098	.023	.153	.504
1.2	-.886	.169	.092	-.067	.111	.106	.019	.225	.675
1.6	-.812	.201	.069	-.053	.155	.113	.015	.294	.803
2.0	-.727	.224	.050	-.041	.202	.118	.011	.360	.897
2.4	-.634	.241	.036	-.031	.250	.122	.006	.422	.965
2.8	-.535	.253	.025	-.023	.299	.124	.002	.480	1.013
3.2	-.432	.262	.017	-.017	.348	.124	-.002	.535	1.046
3.6	-.326	.267	.011	-.013	.398	.122	-.005	.586	1.068
4.0	-.218	.270	.006	-.009	.446	.120	-.008	.633	1.082
4.4	-.110	.272	.003	-.007	.494	.116	-.010	.676	1.089
4.8	-.001	.273	.001	-.005	.539	.112	-.012	.715	1.092
5.2	.109	.273	-.001	-.004	.583	.107	-.014	.751	1.092
5.6	.218	.272	-.002	-.002	.624	.101	-.015	.783	1.090
6.0	.327	.272	-.003	-.002	.664	.095	-.016	.812	1.086
6.4	.435	.270	-.003	-.001	.700	.088	-.016	.838	1.081
6.8	.543	.269	-.004	-.001	.734	.082	-.016	.861	1.076
7.2	.650	.267	-.004	0	.766	.076	-.016	.882	1.070
8.0	.863	.264	-.004	0	.821	.063	-.015	.916	1.058
8.8	1.073	.261	-.004	0	.867	.051	-.014	.941	1.046
9.6	1.281	.259	-.003	.001	.903	.040	-.012	.960	1.035
10.4	1.488	.256	-.003	.001	.932	.031	-.011	.973	1.026
11.2	1.692	.255	-.002	.001	.953	.023	-.009	.983	1.018
12.0	1.895	.253	-.002	.001	.969	.017	-.007	.989	1.012
12.8	2.097	.252	-.001	0	.980	.012	-.005	.993	1.008
13.6	2.298	.251	-.001	0	.988	.008	-.004	.996	1.005
14.4	2.499	.251	-.001	0	.993	.005	-.003	.997	1.002
15.2	2.700	.250	0	0	.997	.003	-.002	.999	1.001
16.0	2.900	.250	0	0	.999	.002	-.001	.999	1.000
16.8	3.099	.250	0	0	1.001	.001	-.001	.999	.999
17.6	3.299	.250	0	0	1.002	.001	-.001	1.000	.998
18.4	3.499				1.002	0	0	1.000	
19.2	3.698				1.002	0	0	1.000	
20.0	3.898				1.002	0	0	1.000	

TABLE I - VELOCITY, WEIGHT-FLOW, AND TEMPERATURE DISTRIBUTIONS  
IN LAMINAR BOUNDARY LAYER WITH VARIABLE FLUID PROPERTIES,  
PRESSURE GRADIENT IN MAIN STREAM, AND FLOW  
THROUGH POROUS WALL - Concluded

$$(12) T_{\infty}/T_w = 4; Eu = 1; f_w = -1.0$$



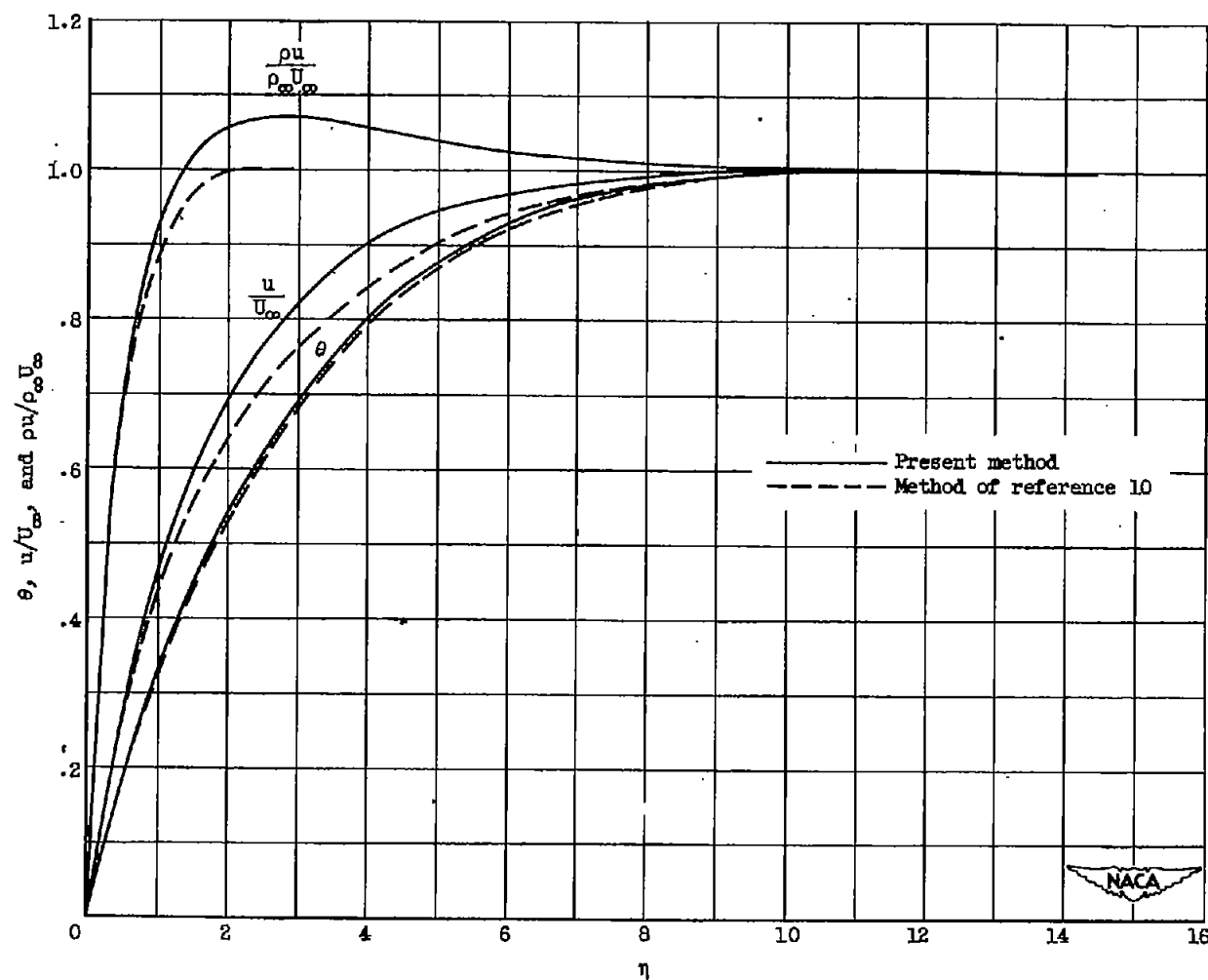
$$\frac{\delta^* \sqrt{Re}}{x} = -0.117; \frac{\delta_i \sqrt{Re}}{x} = 2.602; \frac{\delta_c \sqrt{Re}}{x} = 4.147; \frac{\delta_t \sqrt{Re}}{x} = 4.448$$

$\eta$	$f$	$f'$	$f''$	$f'''$	$\theta$	$\theta'$	$\theta''$	$\frac{u}{U_{\infty}}$ $Pf'$	$\frac{\rho u}{\rho_{\infty} U_{\infty}}$ $4f'$
0	-1.000	0	0.261	-0.142	0	0.073	0.037	0	0
.2	-.995	.049	.232	-.146	.015	.080	.039	.052	.197
.4	-.981	.093	.203	-.144	.032	.088	.039	.102	.371
.6	-.958	.131	.175	-.138	.050	.096	.038	.150	.522
.8	-.929	.163	.148	-.128	.070	.103	.037	.197	.652
1.0	-.894	.190	.124	-.116	.092	.110	.034	.242	.760
1.2	-.853	.213	.102	-.102	.114	.117	.032	.286	.850
1.4	-.809	.231	.083	-.089	.138	.123	.028	.327	.924
1.6	-.761	.246	.066	-.076	.164	.128	.024	.367	.984
1.8	-.711	.258	.052	-.064	.190	.133	.020	.404	1.031
2.0	-.658	.267	.041	-.054	.217	.136	.016	.441	1.068
2.4	-.549	.280	.023	-.036	.272	.141	.009	.508	1.118
2.8	-.435	.286	.011	-.024	.329	.143	.001	.569	1.145
3.2	-.320	.289	.003	-.015	.386	.143	-.005	.624	1.156
3.6	-.205	.289	-.002	-.010	.443	.140	-.010	.673	1.157
4.0	-.089	.288	-.005	-.006	.498	.135	-.014	.718	1.152
4.4	.026	.286	-.006	-.003	.550	.129	-.017	.757	1.143
4.8	.140	.283	-.007	-.001	.600	.121	-.019	.793	1.132
5.2	.252	.280	-.008	0	.647	.113	-.021	.824	1.120
5.6	.364	.277	-.008	0	.691	.105	-.022	.851	1.108
6.0	.474	.274	-.007	.001	.731	.096	-.022	.875	1.096
6.4	.583	.271	-.007	.001	.767	.087	-.022	.896	1.085
6.8	.691	.268	-.006	.001	.800	.078	-.021	.913	1.074
7.2	.798	.266	-.006	.001	.830	.070	-.021	.928	1.064
8.0	1.009	.262	-.005	.001	.879	.054	-.018	.952	1.047
8.8	1.216	.258	-.004	.001	.917	.041	-.016	.969	1.033
9.6	1.422	.256	-.003	.001	.945	.029	-.013	.980	1.022
10.4	1.625	.254	-.002	.001	.965	.020	-.010	.987	1.014
11.2	1.828	.252	-.002	.001	.978	.014	-.007	.992	1.008
12.0	2.029	.251	-.001	0	.987	.009	-.005	.994	1.004
12.8	2.229	.250	-.001	0	.993	.005	-.003	.995	1.000
13.6	2.429	.250	-.001	0	.996	.003	-.002	.995	.998
14.4	2.629	.249	0	0	.998	.002	-.001	.995	.997
15.2	2.828	.249	0	0	.999	.001	-.001	.995	.996
16.0	3.027	.249	0	0	1.000	.001	0	.995	.995
16.8	3.226				1.000	0	0	.995	
17.6	3.425				1.000	0	0	.995	
18.4	3.624				1.000	0	0	.995	

TABLE II - SUMMARY OF HEAT-TRANSFER AND FRICTION  
 PARAMETERS AND BOUNDARY-LAYER THICKNESSES<sup>1</sup>

$f_w$	$\frac{T_\infty}{T_w}$	Eu	$\frac{Nu}{\sqrt{Re}}$ $\theta'_w$	$\frac{C_{f,w}\sqrt{Re}}{2}$ $f_w''$	$\delta \frac{\sqrt{Re}}{x}$	$\delta_1 \frac{\sqrt{Re}}{x}$	$\delta_c \frac{\sqrt{Re}}{x}$	$\delta_t \frac{\sqrt{Re}}{x}$
0	1	-0.0904	0.1993	0	3.498	0.868	0.626	2.737
		-.0868	.2215	.0581	2.971	.852	.692	2.505
		-.0826	.2310	.0870	2.783	.838	.720	2.415
		-.0741	.2435	.1296	2.510	.812	.752	2.307
		-.0654	.2528	.1637	2.336	.788	.773	2.233
		-.0476	.2673	.2202	2.092	.747	.801	2.128
		0	.2927	.3320	1.721	.662	.835	1.959
		.50	.4162	.8997	.855	.377	.792	1.407
		1.00	.4958	1.2326	.648	.290	.708	1.187
		2	-0.1178	0.1890	4.582	1.663	1.076	3.721
		-.09	.2522	.1634	2.430	1.501	1.408	2.928
		-.05	.2756	.2434	1.882	1.378	1.478	2.713
		0	.2944	.3125	1.537	1.271	1.495	2.547
		.50	.4020	.6836	.822	.838	1.372	1.904
		1.00	.4760	.9090	.433	.693	1.215	1.611
		4	-0.1351	0.1794	6.950	3.109	1.834	5.596
		-.09	.2642	.1934	2.297	2.719	2.595	4.053
		-.05	.2790	.2397	1.810	2.582	2.651	3.863
		0	.2952	.2874	1.438	2.455	2.663	3.678
		.50	.3940	.5541	.272	1.676	2.399	2.790
		1.00	.4662	.7220	.081	1.403	2.113	2.370
	-1/2	1	-0.0418	0.1029	4.272	0.954	0.807	3.677
		0	.1661	.1648	2.459	.827	.974	2.650
		.50	.2594	.6974	1.033	.443	.994	1.776
		1.00	.2934	.9692	.783	.345	.918	1.530
		2	0	0.1602	2.381	1.605	1.778	3.456
		.50	.2304	.4770	.772	1.044	1.771	2.476
		1.00	.2560	.6415	.507	.880	1.638	2.151
		4	-0.0644	0.0796	7.219	3.485	2.620	7.329
		0	.1506	.1263	2.460	3.100	3.237	5.012
		.50	.2088	.3448	.318	2.155	3.142	3.870
		1.000	.2252	.4465	0	1.867	2.932	3.233
		-1	-0.0072	0.0251	6.398	1.116	1.072	5.997
		0	.0516	.0355	4.396	1.073	1.150	4.414
		.05	.0881	.1410	2.796	.911	1.241	3.317
		.15	.1129	.2703	2.008	.750	1.280	2.806
		.50	.1392	.5344	1.252	.525	1.270	2.274
		1.00	.1457	.7565	.945	.405	1.208	1.995
		2	0	0.0406	4.931	2.114	2.167	5.941
		.05	.0692	.0892	2.985	1.911	2.299	4.625
		.15	.0886	.1678	1.989	1.704	2.343	3.959
		.50	.1062	.3228	.965	1.310	2.298	3.236
		1.00	.1052	.4445	.608	1.148	2.228	2.891
		4	0	0.0262	6.409	4.160	4.002	9.007
		.05	.0510	.0542	3.405	3.881	4.247	6.995
		.15	.0656	.1030	2.040	3.620	4.309	6.054
		.50	.0780	.1959	.402	2.882	4.256	4.954
		1.00	.0726	.2611	.117	2.602	4.147	4.448
0	1/2	-0.06	0.2062	0	3.043	0.442	0.348	2.215
		-0.04	.2554	.1735	2.309	.406	.420	1.846
		0	.2900	.3482	1.898	.347	.457	1.645
		.50	.4412	1.2754	.980	.116	.460	1.109
		1.00	.5298	1.8000	.768	.065	.415	.929
	1/4	0	0.2884	0.3556	2.031	0.182	0.246	1.482
		1/2	.4801	1.9299	1.033	-.031	.270	.919
		1	.5812	2.7842	.820	-.064	.246	.764

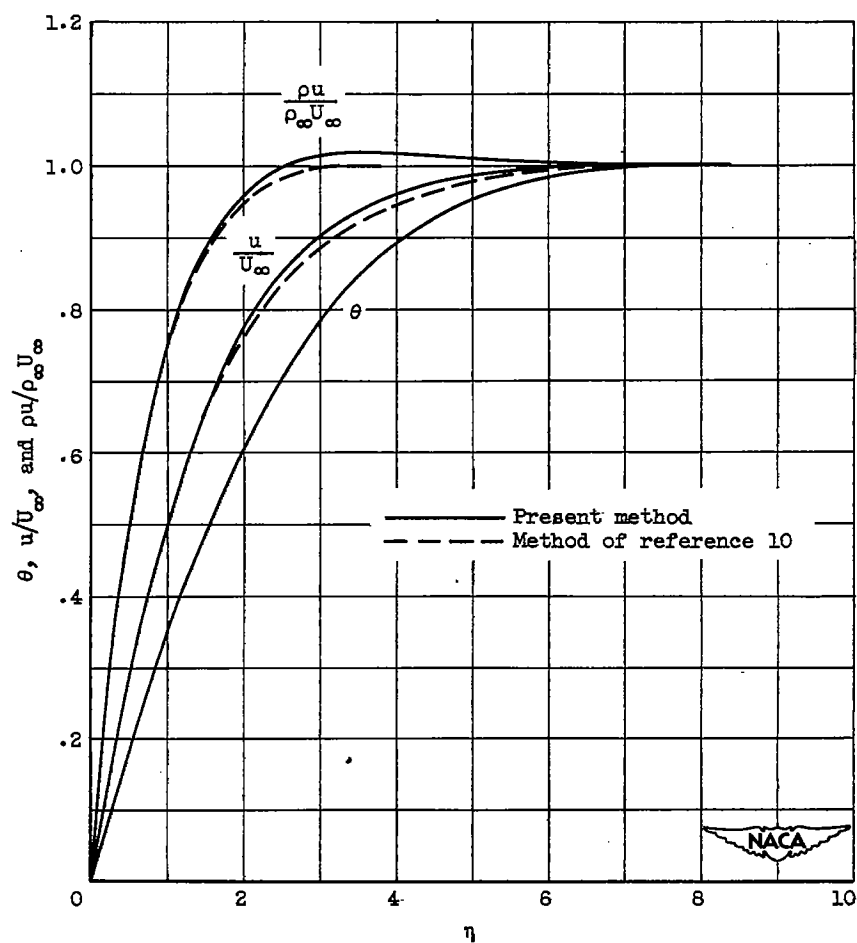
<sup>1</sup>The last figure in the boundary-layer thicknesses is doubtful.



(a) Impermeable wall; Euler number, 1; stream-to-wall temperature ratio, 4.

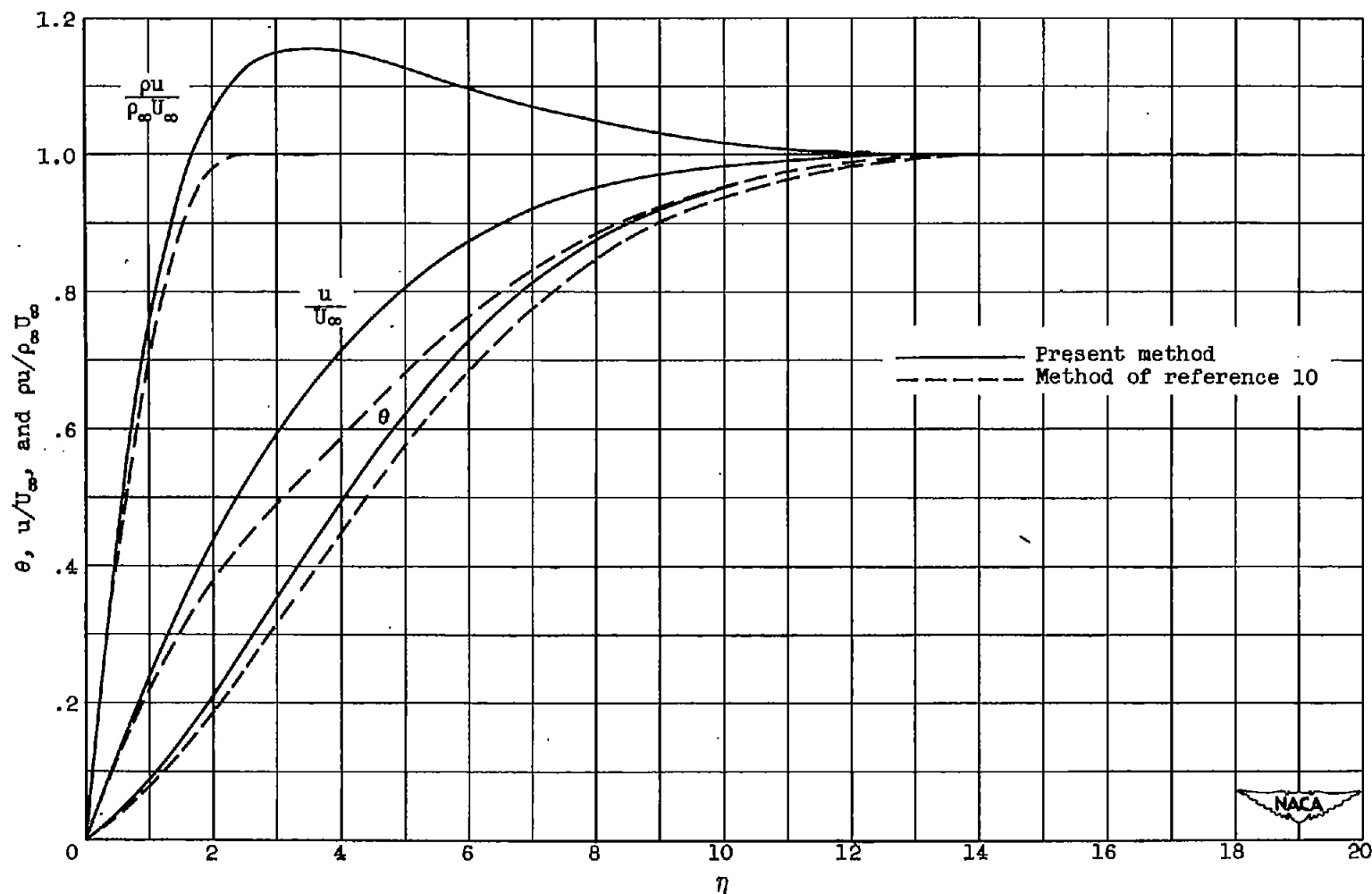
Figure 1. - Specific-weight-flow, velocity, and temperature profiles through boundary layer.





(b) Impermeable wall; Euler number,  $1/2$ ; stream-to-wall temperature ratio, 2.

Figure 1. - Continued. Specific-weight-flow, velocity, and temperature profiles through boundary layer.



(c) Flow rate through porous wall, -1; Euler number, 1; stream-to-wall temperature ratio, 4.

Figure 1. - Concluded. Specific-weight-flow, velocity, and temperature profiles through boundary layer.

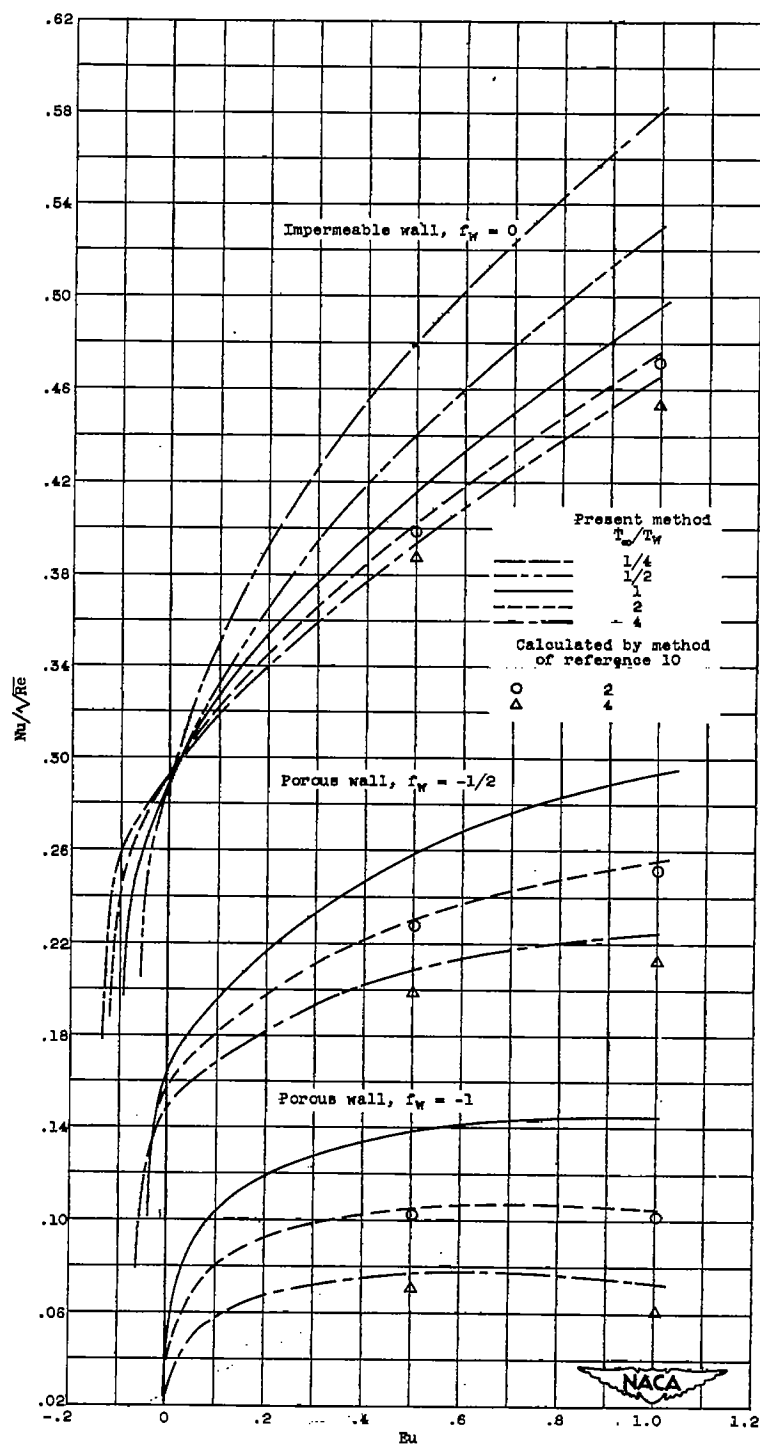
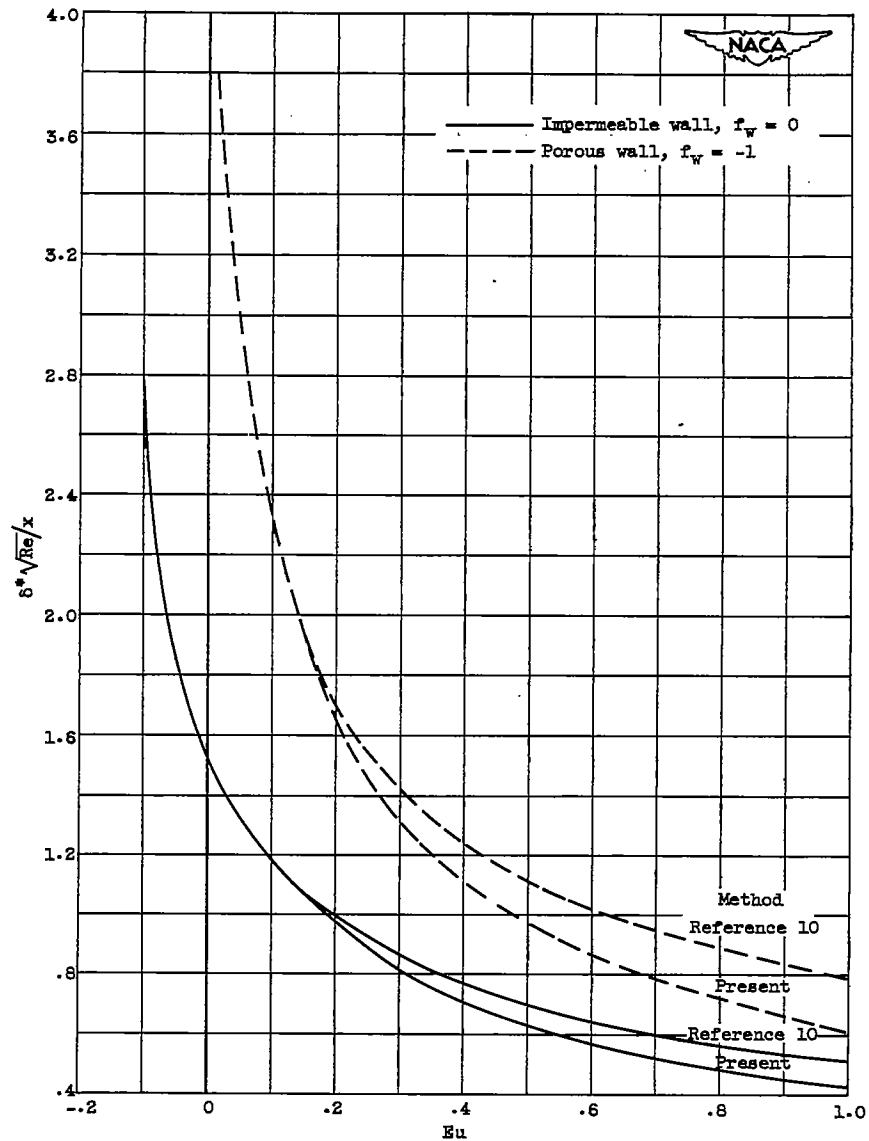
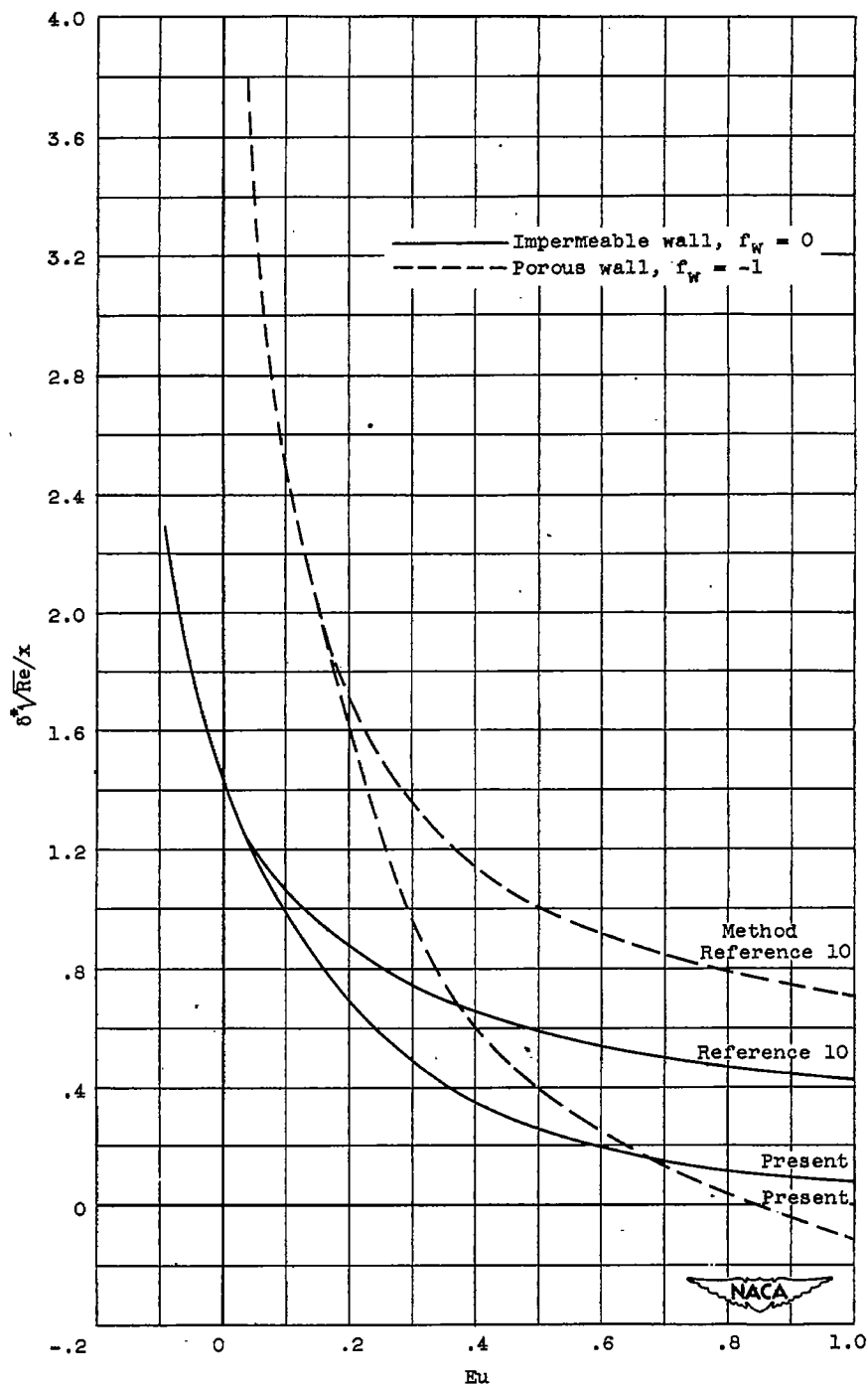


Figure 2. - Heat transfer through laminar boundary layer with and without flow through porous wall.



(a) Stream-to-wall temperature ratio, 2.

Figure 3. - Nondimensional displacement thickness with and without porous flow.



(b) Stream-to-wall temperature ratio, 4.

Figure 3. - Concluded. Nondimensional displacement thickness with and without porous flow.